

## Introduction

Since 2011, graduate students and faculty at the University of Oklahoma have used RaXPol (Pazmany et al. 2013) – a rapid-scan, polarimetric, mobile radar – to collect data of tornadoes, supercells, and related phenomena in the central United States. On 31 May 2013, RaXPol sampled a multiple-vortex tornado in El Reno, OK, with radial velocities ( $V_R$ ) exceeding  $135 \text{ m s}^{-1}$ . Several of the observed subvortices moved at speeds of  $75\text{--}80 \text{ m s}^{-1}$ , limiting the duration of time the extraordinarily strong winds were experienced at any one location. There is great uncertainty, however, regarding how the observed  $V_R$  relates to a 3 second,  $\sim 10 \text{ m AGL}$  wind speed standard such as that used in the Enhanced Fujita (EF) Scale. In addition, differential radial velocity ( $V_D$ ), defined as the difference between the  $V_R$  calculated using the H channel ( $V_H$ ) and that calculated using the V channel ( $V_V$ ), within several intense tornadoes is shown. Large  $V_D$  tends to be associated with high  $\sigma_v$  and low  $\rho_{hv}$ , not surprising given the increased variance in the velocity estimates expected when those two conditions are observed. More details and discussion of these data can be found in Snyder and Bluestein (2014).

## What does a $V_R$ observation represent?

The  $V_R$  estimate at a given range gate represents the reflectivity-weighted average velocity of all scatterers within a radar resolution volume during a given integration period (i.e., dwell time) towards or away from the radar. How does this relate to a 3 s, 10 m AGL wind speed standard?

- $V_R$  estimate** – Many pulsed Doppler weather radars use pulse-pair processing to calculate  $V_R$ , which often requires assumptions to be made about the shape of the power spectrum. The quality of the estimate is affected by factors such as the number and independence of samples used and the width of the power spectrum.
- Reflectivity-weighted average velocity** –  $V_R$  estimates are typically biased towards the largest and/or most abundant scatterers being sampled. Typically, in high acceleration flows such as tornadoes, the peak velocity of the more massive objects is likely to be less than the peak velocity of the wind.
- Within a radar resolution volume** – The size of the volume illuminated by the antenna is affected by the distance from the radar, the transmitted pulse width, and the antenna's radiation pattern. An antenna with a 3 dB beamwidth of  $1^\circ$  has a cross-sectional width of  $\sim 87 \text{ m}$ ,  $\sim 260 \text{ m}$ , and  $\sim 525 \text{ m}$  at 5, 15, and 30 km ranges, respectively. It's highly likely that the peak velocity of scatterers being sampled exceeds the mean velocity owing to spatial averaging. In addition, owing to beam broadening, partial beam blockage, and potential multipath scattering, the illuminated radar volume is likely to be quite complex for elevation angles near  $0^\circ$ , making it extremely difficult to sample near the ground.
- During a given integration period** – the data that are used to calculate commonly-used radar quantities at each range gate are typically collected very quickly (i.e., dwell time per radial of  $\sim 0.005\text{--}0.05 \text{ s}$ ), so the calculated  $V_R$  data are nearly instantaneous velocities.
- Towards or away from the radar** – Modeling and theory suggest that, within some tornadoes, the vertical component of the velocity may be similar to (or even exceed) the horizontal component. As such, minor deviations of elevation angle from true horizontal will result in an increasing contribution to the measured  $V_R$  from the vertical velocity.

	RaXPol
Wavelength	$\sim 3.1 \text{ cm}$ (9.73 GHz $\pm$ 20 MHz)
Transmit Power	Peak: 20,000 W Average: 200 W
Polarization	Simultaneous linear H and V
Range Resolution	15 – 150 m
Range Gate Spacing	7.5 – 75 m
Antenna Diameter	2.4 m
3 dB Beamwidth	1.0 deg.
Max. Antenna Scanning Rate	Azimuth: $\sim 180 \text{ deg. s}^{-1}$ Elevation: $\sim 24 \text{ deg. s}^{-1}$

Table 1. Selected characteristics of the radar system used in this project.

## 31 May 2013



Fig. 1. A map of the RaXPol deployments near El Reno, Oklahoma, on 31 May 2013. The orange swath marks the track of the main "El Reno" tornado; the yellow curve marks an anticyclonic tornado track. A brief, weak tornado occurred before the primary cyclonic tornado began and is marked in light blue.

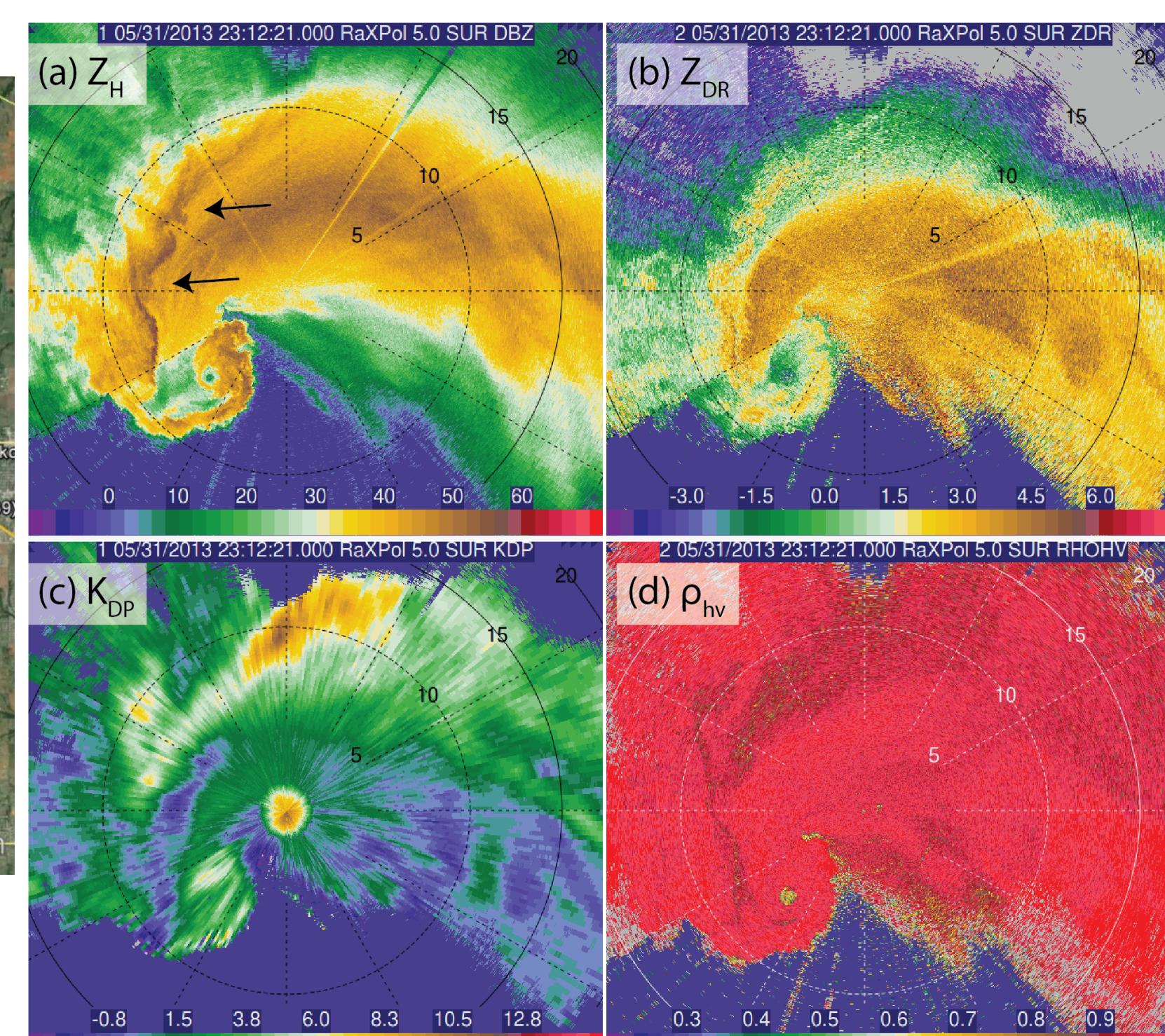


Fig. 2. RaXPol data from the second deployment location in southwestern El Reno as a tornadic supercell approached.

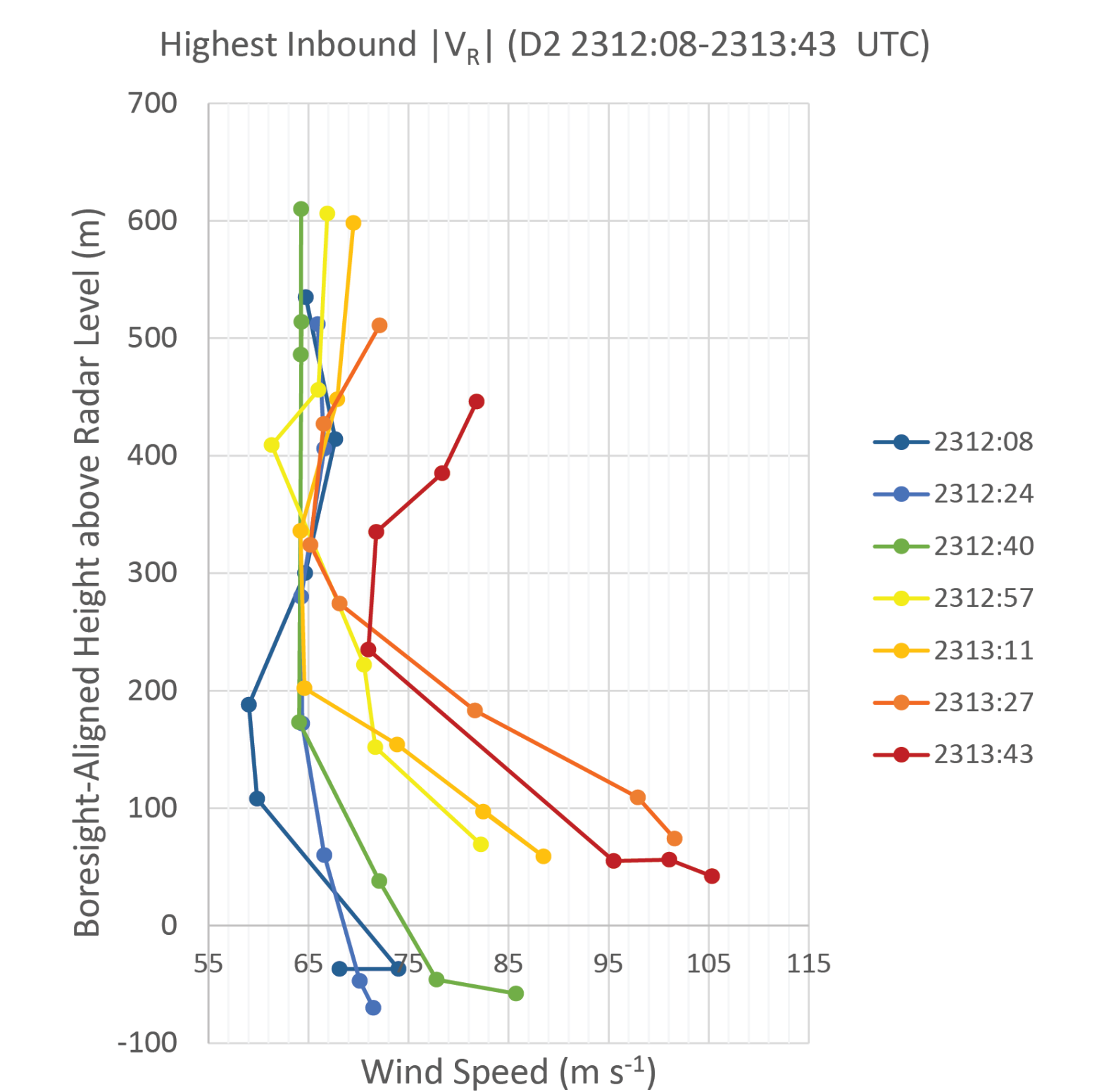


Fig. 3. The vertical profile of maximum  $|V_R|$  at the end of the second deployment.

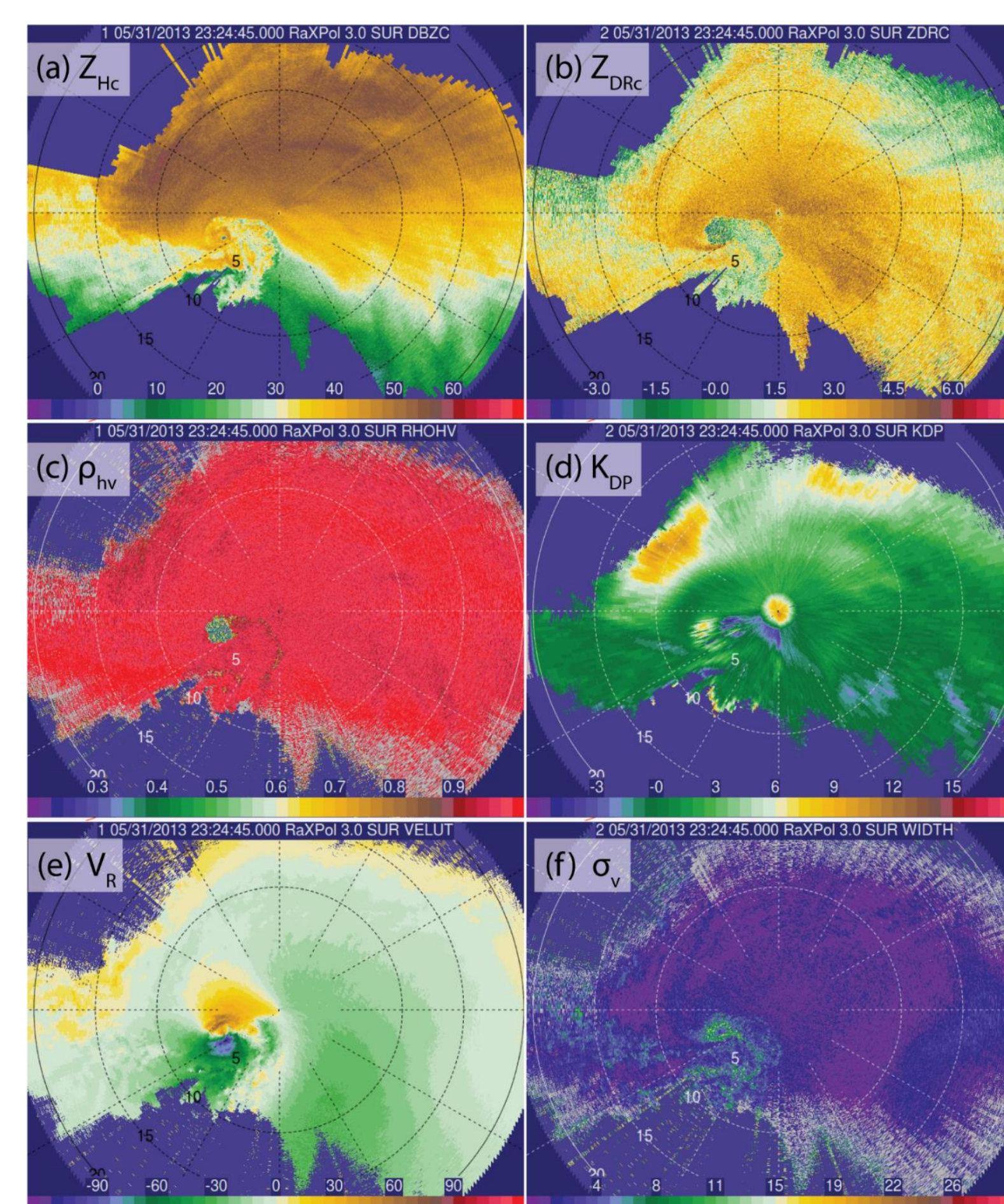


Fig. 5. A "zoomed out" view of the supercell near the start of the third deployment. Estimated attenuation by rain has been corrected for in (a) and (b).

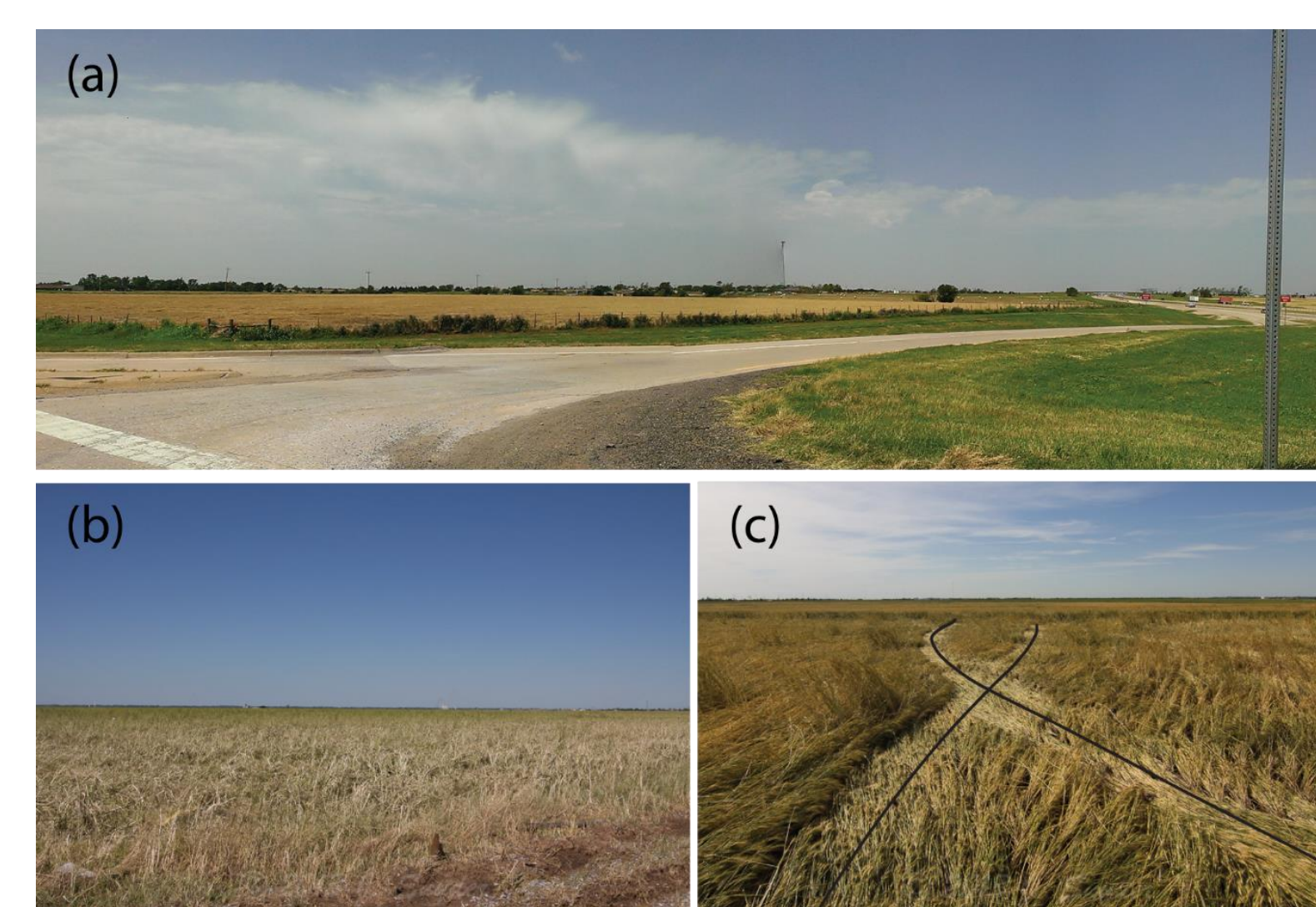


Fig. 6. Photographs from (a) near the third deployment location, (b) the field in which RaXPol sampled  $V_R$  of at least  $135 \text{ m s}^{-1}$ , and (c)  $< 1 \text{ m}$  wide, helical swaths of matted vegetation in the same field. Photographs courtesy J. Snyder.

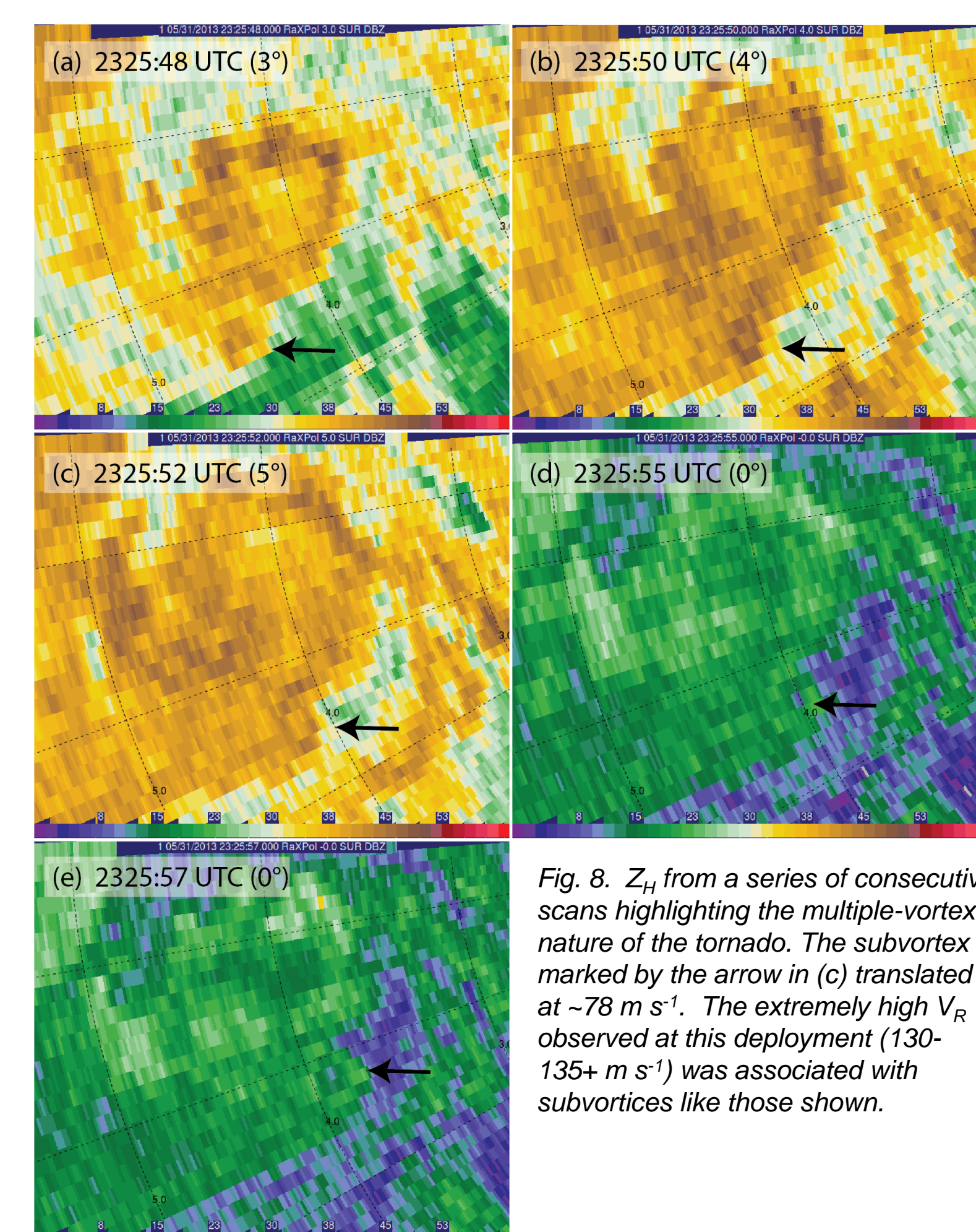


Fig. 8.  $Z_H$  from a series of consecutive scans highlighting the multiple-vortex nature of the tornado. The subvortex marked by the arrow in (c) translated at  $\sim 78 \text{ m s}^{-1}$ . The extremely high  $V_R$  observed at this deployment ( $130\text{--}135\text{+} \text{ m s}^{-1}$ ) was associated with subvortices like those shown.



Fig. 4. Photographs of the extremely large tornado in El Reno, Oklahoma, from RaXPol's third deployment location. The red circles in (a)–(b) mark the approximate size of the 3 dB beamwidth at the range of the tornado (3–5 km), and the white arrow in (c) points to RaXPol. Photographs (a)–(c) courtesy of J. Snyder, H. Bluestein, and G. Rhoaden, respectively.

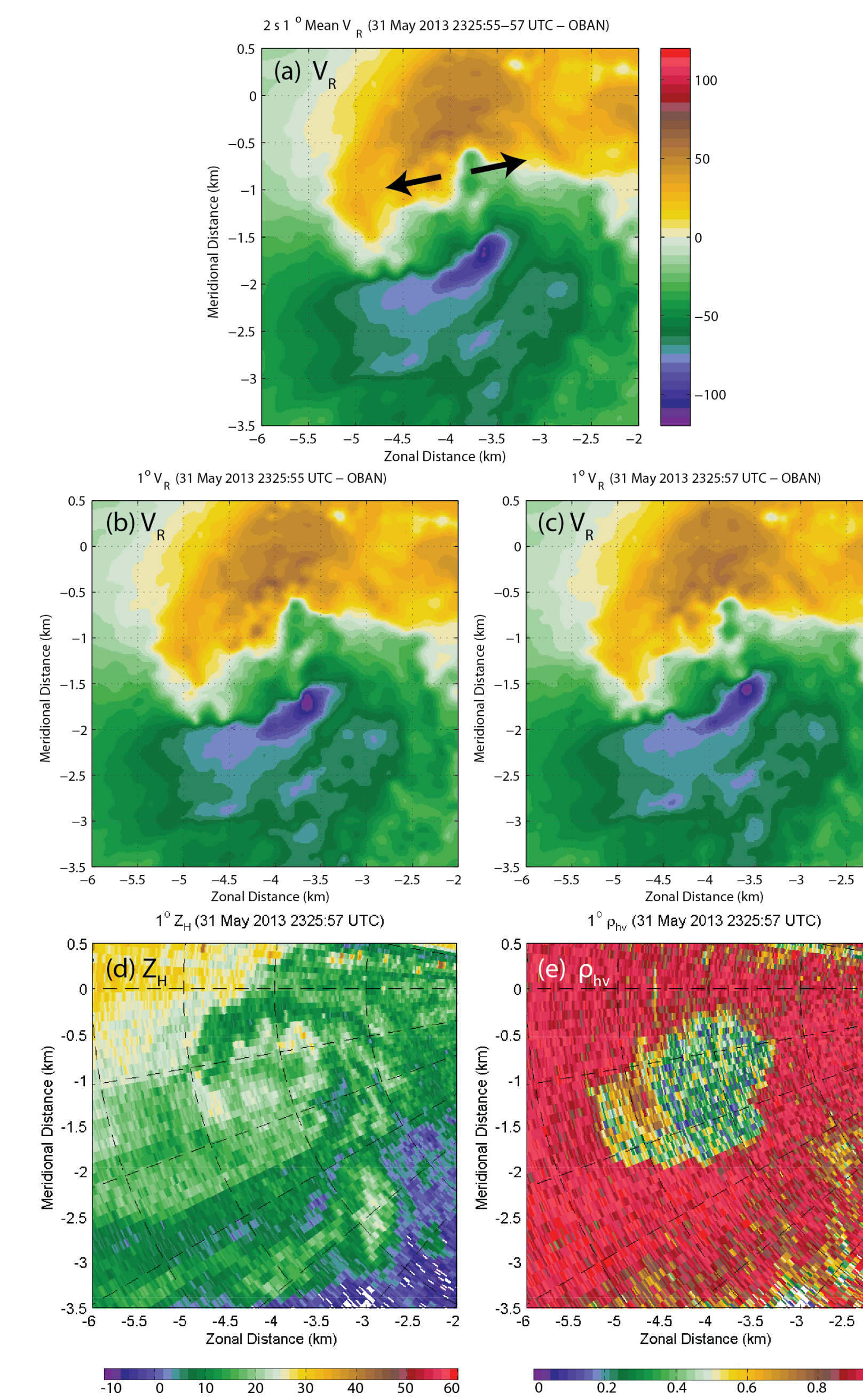


Fig. 7. (Left) RaXPol is currently configured to scan the lowest elevation angle of a volume scan twice, which means that the  $0.0^\circ$  elevation angle was scanned at a 2-s interval at every  $\sim 16 \text{ s}$  during the latter part of the second and during the entire third deployment. As a result, we can average the two scans to estimate a 2-s average  $V_R$ , which reduces one of the primary sources of uncertainty when relating radar observations to the EF Scale. In this case, peak inbound  $V_R$  from two consecutive scans (b) and (c) is  $119.5$  and  $116.4 \text{ m s}^{-1}$ ; the peak 2-s averaged  $V_R$  is  $109.3 \text{ m s}^{-1}$ .

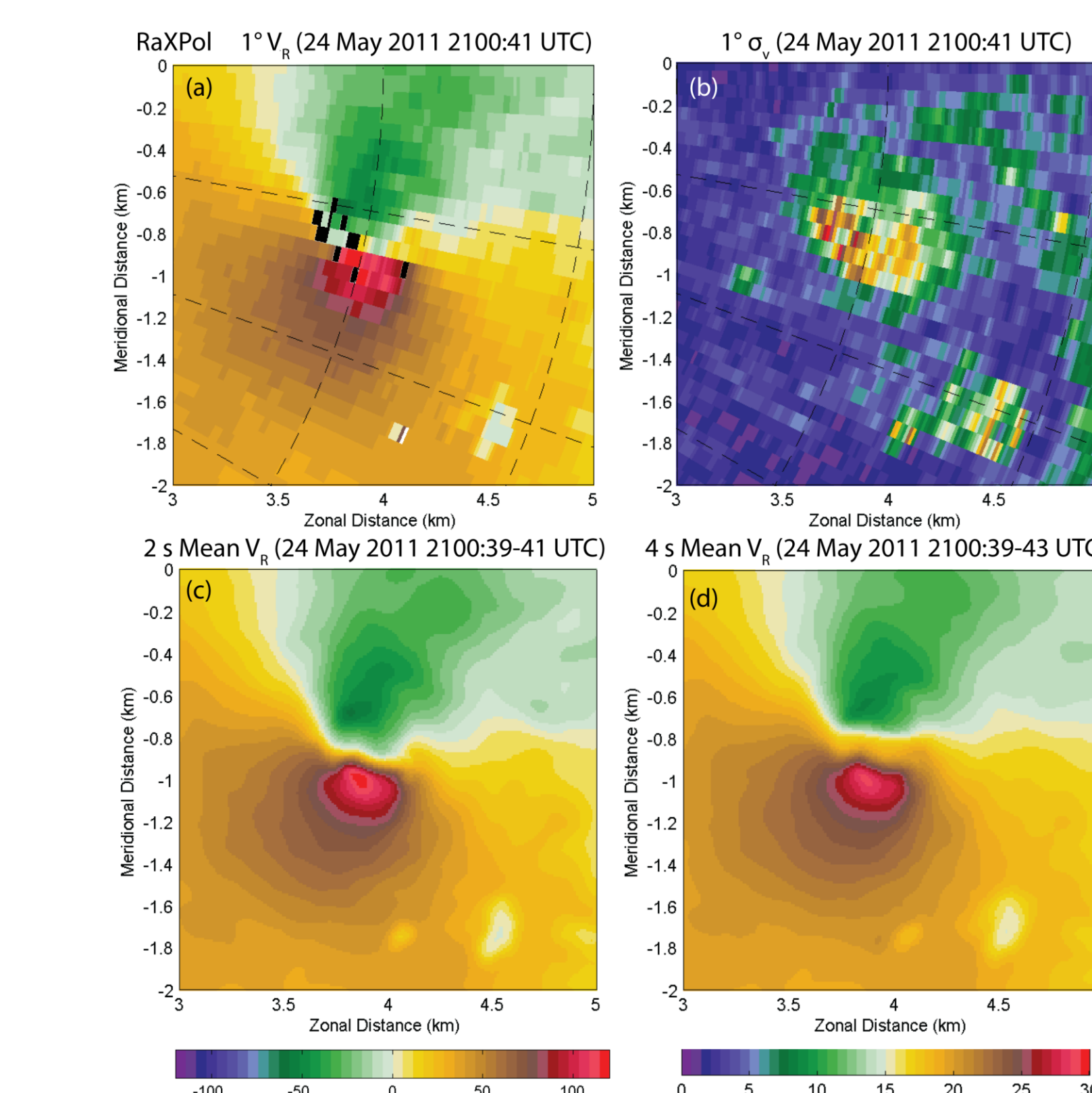


Fig. 9. On 24 May 2011, a violent tornado near El Reno, OK, passed  $\sim 2.5 \text{ km}$  southeast of RaXPol. The scanning strategy at the times shown above consisted of 2 s PPIs at  $1.0^\circ$  elevation angle, which allows us to estimate the 2 s and 4 s average  $V_R$ . In this case, peak  $V_R$  in (a) is  $132.1 \text{ m s}^{-1}$ , peak  $V_V$  in the objectively analyzed data at this time (not shown) is  $129.4 \text{ m s}^{-1}$ ; the peak in the (c) 2 s and (d) 4 s mean  $V_R$  is  $118.4 \text{ m s}^{-1}$  and  $110.8 \text{ m s}^{-1}$ , respectively.

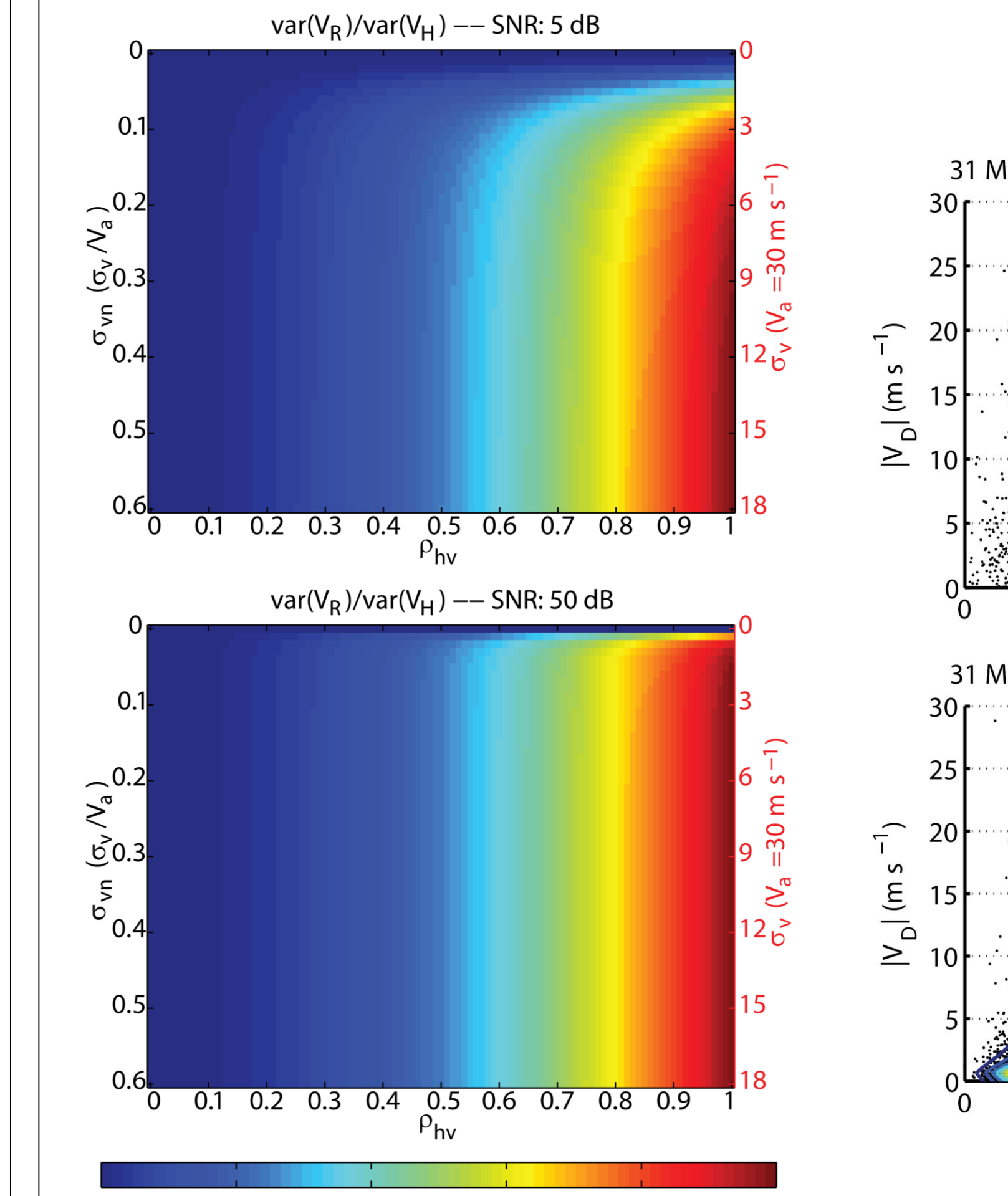


Fig. 10. Where  $\rho_{hv} \sim 1.0$ ,  $V_V$  and  $V_R$  should be very similar since the signals in each channel are highly correlated. In the debris field of a tornado, however,  $\rho_{hv}$  tends to be markedly reduced. In such places, the combination of  $V_V$  and  $V_R$  (or the combination of the autocorrelation functions from H and V) to produce a "polarimetric"  $V_R$  estimate reduces the variance of the velocity estimate. Consequently, polarimetric radars should produce higher-quality  $V_R$  estimates in the presence of debris when compared to single-polarization radars. See Melnikov (2004) for details.

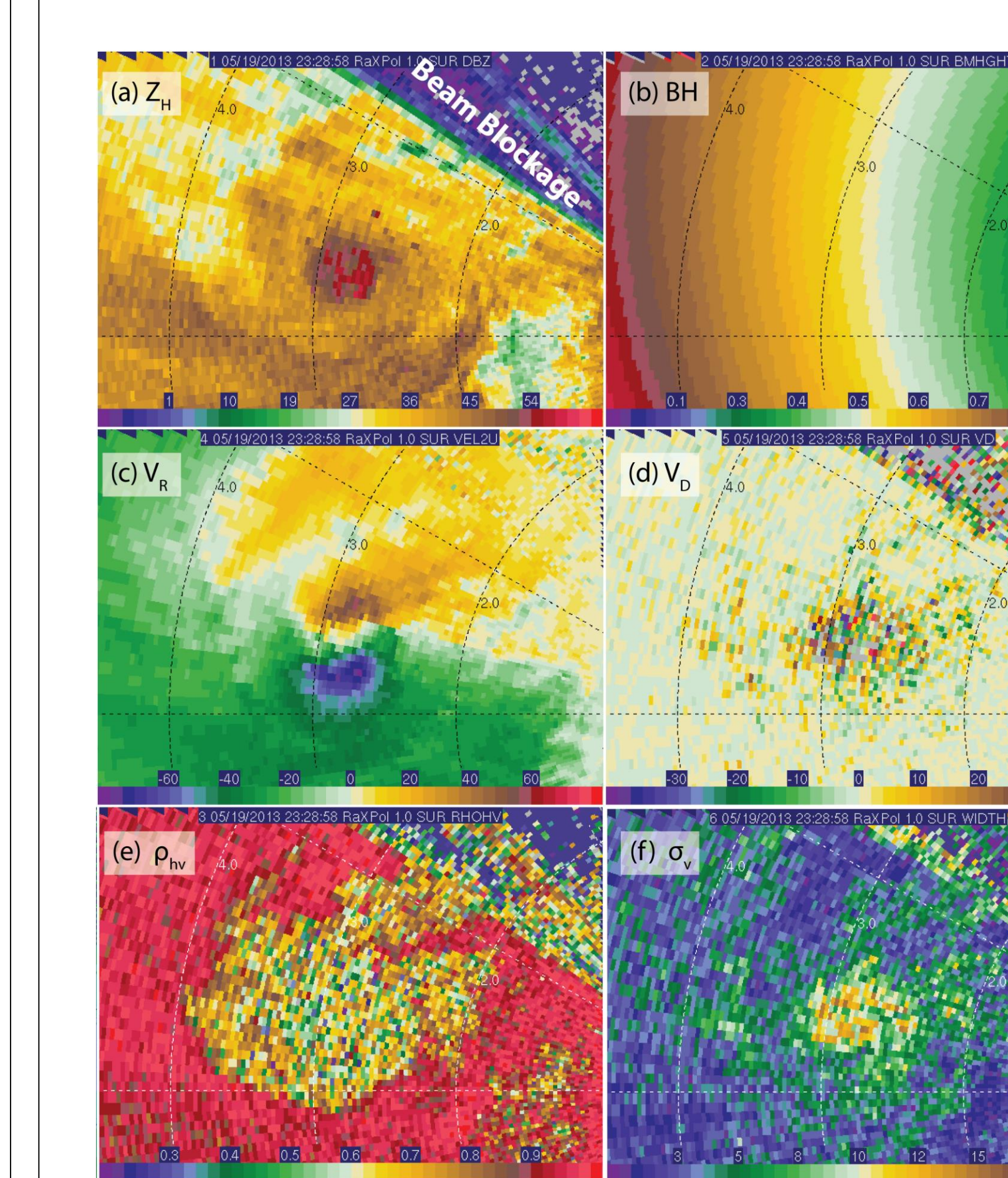
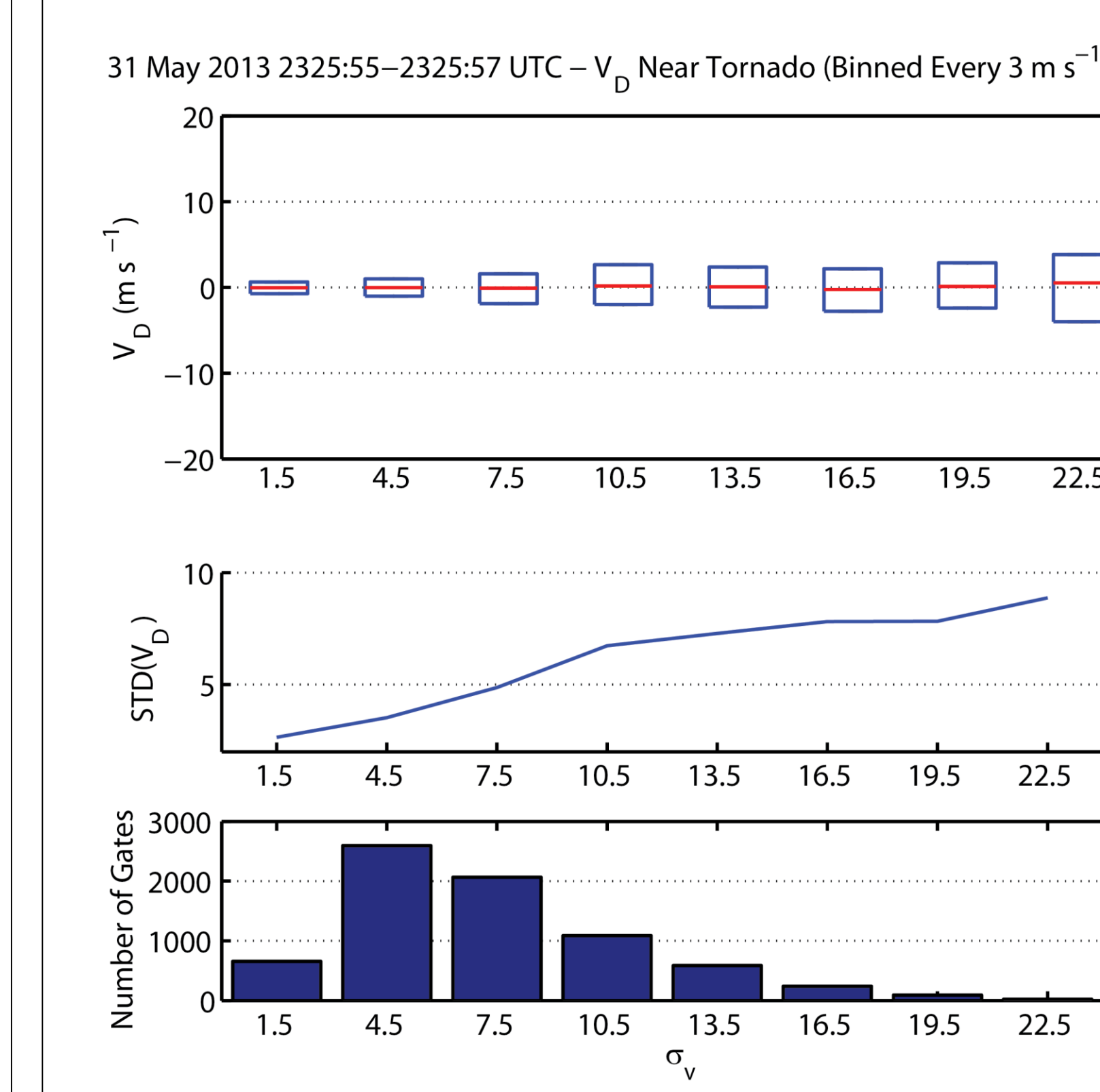


Fig. 14. RaXPol data from the evening of 19 May 2013 sampling a violent tornado centered  $\sim 2.8 \text{ km}$  WNW of the radar. "BH" in (b) represents approximate bore-sight-aligned beam height above radar level after accounting for non-zero pitch and roll.

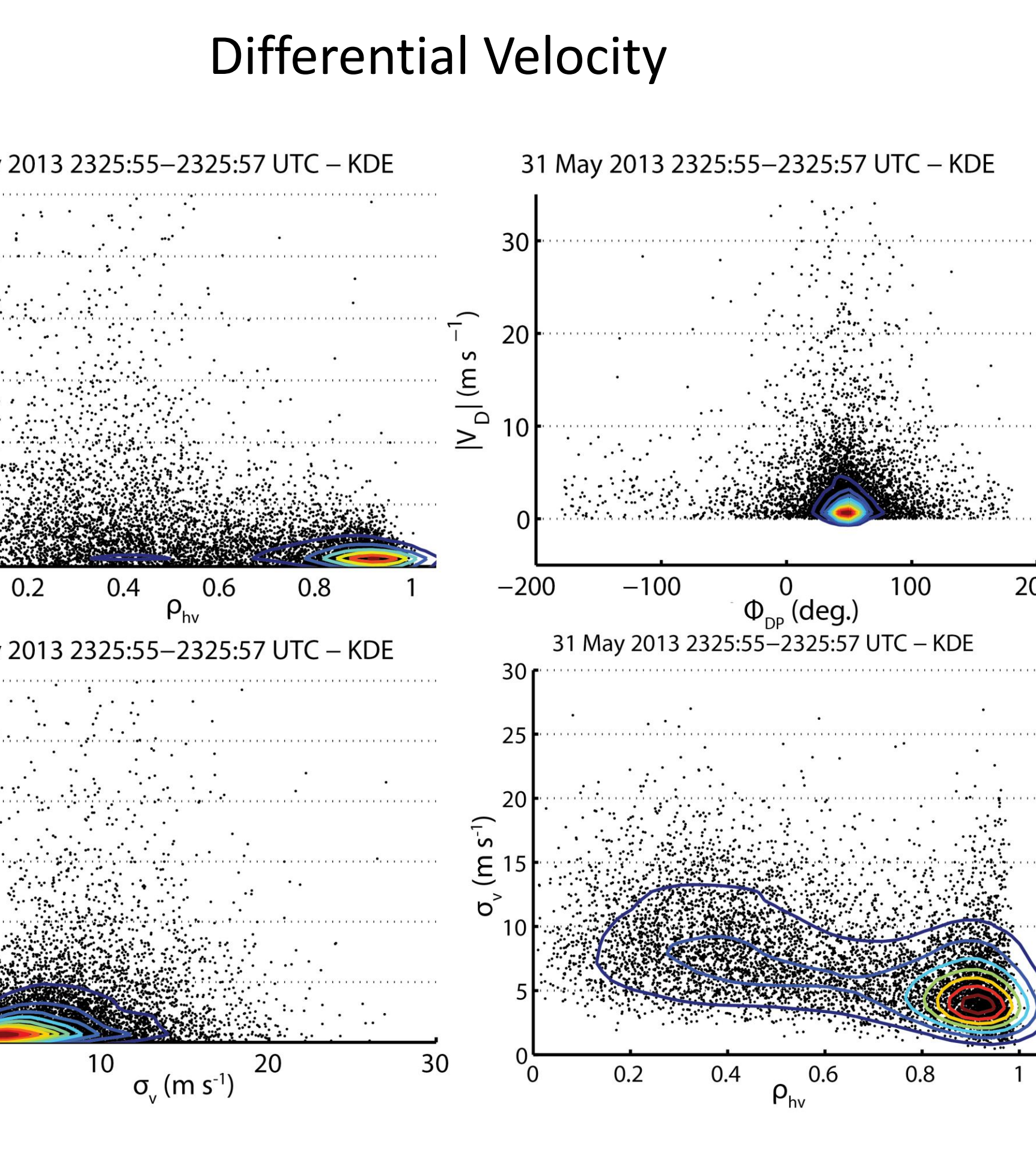


Fig. 11. Scatterplots and kernel density estimates (contoured) of the magnitude of differential velocity ( $V_D$ ) for gates within and immediately surrounding the tornado debris field in two  $0.0^\circ$  elevation angle scans from the third deployment on 31 May 2013.

Fig. 12. (Below left) Median and ranges ( $10^{\text{th}}\text{--}90^{\text{th}}$  percentile) of  $V_D$ , standard deviation of  $V_D$ , and the number of data points for all gates near the tornado on two  $0.0^\circ$  elevation angle scans on 31 May 2013 as a function of spectrum width binned every  $3 \text{ m s}^{-1}$ .

Fig. 13. (Below right) As in Fig. 12, but as a function of  $\rho_{hv}$  binned every 0.1.

## Acknowledgments

This research was performed while the first author held a National Research Council Research Associateship Award at NSSL. The radar and data presented in this project were supported through NSF MRI grant AGS-0821231 and NSF grants AGS-0934307 and AGS-1237404 awarded to the University of Oklahoma. The authors wish to thank Jana Houser and Vivek Mahale for helping to collect some of the data presented in this paper. Discussions with Valery Melnikov were quite insightful.